Available online at www.sciencedirect.com
SCIENCE DIRECT®
Applied Energy 81 (2005) 260–276
APPLIED ENERGY
www.elsevier.com/locate/apenergy

Improvement of a chain-hardening furnace by computational fluid dynamics (CFD) simulation

J.M. Sala [a], L.M. López González [b,*], J.L. Míguez [c], J.J. Eguía [a], J.E. Vicuña [b], M.C. Juárez [b], J. Doménech [b]

[a] *E.T.S. Ingenieros Industriales de Bilbao, Alda. Urquijo, s/n, 48013 Bilbao, Spain*
[b] *Grupo de Termodinamica Aplicade, Departamento de Ingenieria Mecanica, Universidad de La Rioja, Escuela Técnica Superior de Ingeniería Industrial de Logroño, C/Luis de Ulloa 20, 26004 Logroño (La Rioja), Spain*
[c] *E.T.S. de Ingenieros Industriales de Vigo, Lagoas-Marcosende, 36200-Vigo, Spain*

Accepted 10 August 2004
Available online 28 October 2004

Abstract

Hardening heat-treatment is an important operation in the fabrication of large chains for both the shipping industry and anchorage of offshore oil-platforms. This paper presents the outcome of an investigation that led to the introduction of modifications in a hardening furnace resulting in a substantial improvement and largely eliminating the problem of gradual cooling of the chain before immersion in the water-quenching tank. Comparing this with the present operating conditions, it can be concluded that redirecting the gas flow increases the gas temperature in the lower part of the furnace, which changes the chain's temperature-distribution accordingly.
© 2004 Elsevier Ltd. All rights reserved.

Keywords: Modelling; Furnace; Chain; CFD

* Corresponding author.
E-mail address: luis-maria.lopez@dim.unirioja.es (L.M.L. González).

0306-2619/$ - see front matter © 2004 Elsevier Ltd. All rights reserved.
doi:10.1016/j.apenergy.2004.08.001

1. Introduction

One of the world's leading manufacturers of chains for the shipping industry and offshore oil-platforms has manufacturing facilities near Bilbao. The facilities are provided with bar-heating furnaces and heat-treatment furnaces. This paper summarises the results of an investigation based on the application of computational fluid

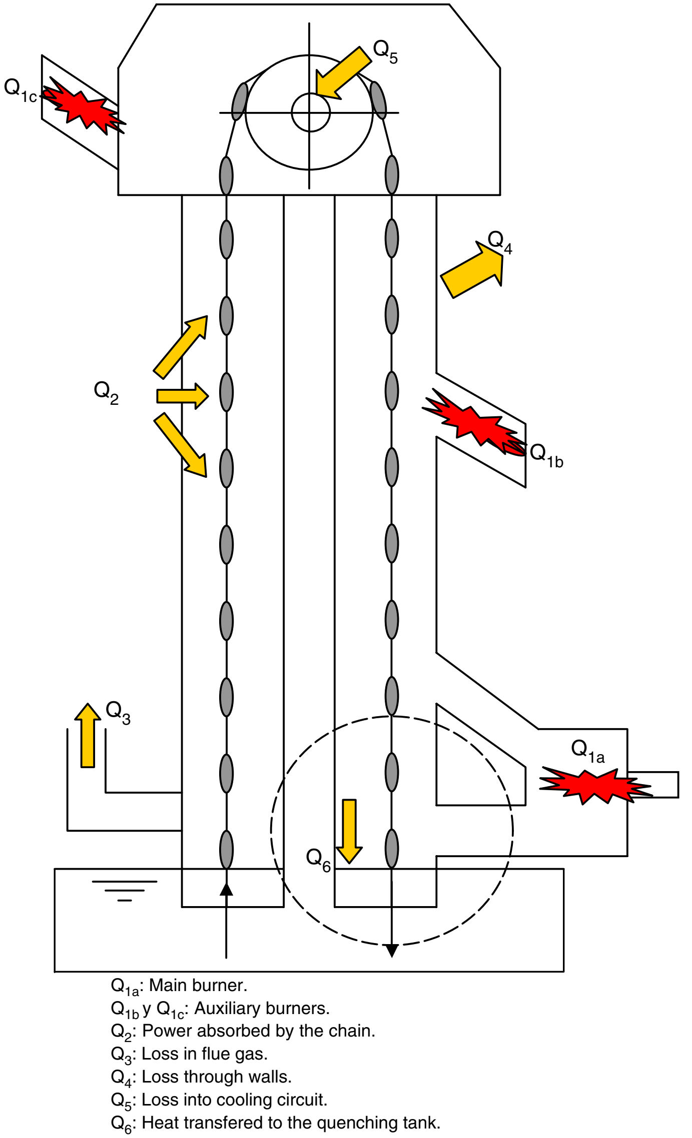

Fig. 1. Schematic drawing of the chain-hardening furnace.

dynamics (CFD) techniques that led to a substantial improvement of the behaviour of the hardening furnace.

The goals of numerical simulation are to improve the design of new or existing furnaces by optimizing the flow distribution. Examples of numerical applications include boilers, burners, ducts [1,2], furnaces [3,4], glass-melting furnaces [5,6], simulation of air flow [7,8] and thermal stratification [9].

The furnace under investigation is of the continuous type, featuring two vertical columns of sufficient length and diameter to allow the chain to move through the inside of the furnace during the time required for the heat-treatment process. It is provided with three natural-gas fired burners: one of the burners, Q_{1a}, with a power of 1400 kW, is located in the main combustion chamber and supplies most of the heat required to heat up the chain. The job of the two other burners, Q_{1b} and Q_{1c}, with a power of 700 kW each, is to supplement the main burner by providing more energy in certain areas. The quenching tank, which contains enough water to cool down the chain, is located below the furnace. Figs. 1–4 depict the furnace geometry and burner locations.

Hardening treatment is carried out by heating the material up to around 950 °C and then cooling it down very quickly by quenching it in water. The moment the chain gets into the water, the water vaporises and the vapour rises through the fur-

Fig. 2. Chain-hardening furnace.

Fig. 3. 3.182 mm chain.

Fig. 4. Test machine.

nace column absorbing heat from the chain. This is why the chain is currently subject to unwanted cooling in the final part of its run before coming into contact with the water, so that it does not reach the required 950 °C.

This means a loss in hardening quality and a solution to the problem has been sought through a detailed analysis of the area where gas ducting from the combustion chamber enters the furnace (the area enclosed by the discontinuous line in Fig. 1) by redirecting the hot gas flow, increasing the velocity of gas circulation in the area, etc.

Given the diversity and complexity of the actual physical phenomena (turbulence, heat transfer with high temperature-gradient, evaporation, etc.) that occur simultaneously inside the furnace, it was decided to apply computational fluid dynamics. CFD allows the aerodynamic behaviour of the gas inside the furnace to be predicted, so that once a simulation has been set up, different solutions can be proposed and the most suitable alternative selected.

In short, the chain-cooling process is analysed in detail through the CFD simulation, determining temperature ranges, gas paths, etc. inside the furnace, with a view to redesigning the area in the vicinity of the quenching tank.

2. Energy audit for the furnace

First, an energy audit was performed to determine the energy-flux distribution in the furnace. A number of temperature and gas composition measurements were taken and furnace surface temperatures were determined by sampling at different points. A furnace diagram is given in Fig. 1. The energy balance is worked out for the control volume of the whole furnace.

- Fuel power supplied ($Q_{1a} + Q_{1b} + Q_{1c}$).

  Apart from the main burner (Q_{1a}) there are two auxiliary burners (Q_{1b} and Q_{1c}), which work intermittently depending on the gas temperatures in two areas of the furnace. From the daily consumption of natural gas under rated conditions, we obtain $Q_{1a} + Q_{1b} + Q_{1c} = 1.199$ kW.
- Power supplied to the chain (Q_2).

  Sixty-four tonnes of chain were treated in one furnace working day, with the temperature being increased from 30 °C to a maximum of 950 °C. Taking into account the specific heat of the chain material, we get $Q_2 = 359$ kW.
- Heat loss in gases ($Q_3 + Q_7$).

  Gas composition and flue-gas temperature readings were taken with a TESTO 350 gas-analyser. The gas flow was determined by measuring gas velocities in various flue sections.

  Gas-leakage losses were determined by taking into account the excess air obtained through the analyser, and a mean temperature assigned. As a result of these calculations and assessments, a final value for the heat loss through flue gases and gas leakage was obtained, i.e., $Q_3 + Q_7 = 703$ kW.
- Heat loss through walls (Q_4).

  To assess the heat loss through the walls, the surface temperature was measured at 16 points, including all four external walls of the furnace enclosure, with the result that $Q_4 = 93$ kW.
- Heat loss through the roller cooling-circuit (Q_5).

The rollers for moving the chain inside the furnace are cooled through a closed-loop water-cooling circuit. From the flow rate and inlet and outlet temperatures, we arrive at $Q_5 = 12$ kW.

- Heat loss into the quench tank (Q_6).

Finally, we obtain the heat given up by the furnace gases to the quenching tank, where the chain is cooled down, i.e., $Q_6 = 32$ kW.

The table below shows these terms and the percentage of total energy consumption represented by each. These values are used to obtain the furnace efficiency, i.e.,

$$\eta_{\text{furnace}} = \frac{Q_2}{Q_1} = 30.0\%$$

Term	kW	%
Q_1, fuel used	1.199	100
Q_2, useful power	359	30.0
$Q_3 + Q_7$, loss in gases	703	58.6
Q_4, loss through walls	93	7.7
Q_5, loss into the cooling circuit	12	1.0
Q_6, loss into the quenching tank	32	2.7

3. Construction of the mathematical model

3.1. Geometry

Only the column down which the chain moves is considered. There are three hot-gas intakes in the furnace area considered: the two lower intakes come from the main combustion chamber Q_{1a} and the auxiliary burner Q_{1b} and the upper intake from the auxiliary burner Q_{1c}.

3.2. Gridwork

Hexahedron elements have been selected for the chain area, and the selected MAP diagram provides an excellent grid quality: 4480 elements are used.

A hybrid grid, comprising hexahedron and tetrahedron type elements, is used in the gas domain. In this case, the domain is divided into different areas to allow adequate gridwork, with different grid schemes used in each area (COOPER, T-GRID and MAP). The number of elements is 104,160. Fig. 5 shows the gridwork of the area above the quenching tank.

3.3. Gas intakes

An intake velocity of 10 m/s with a flow direction perpendicular to the intake is selected. Gas temperature at the intake is approximately 1300 K; the gas being a

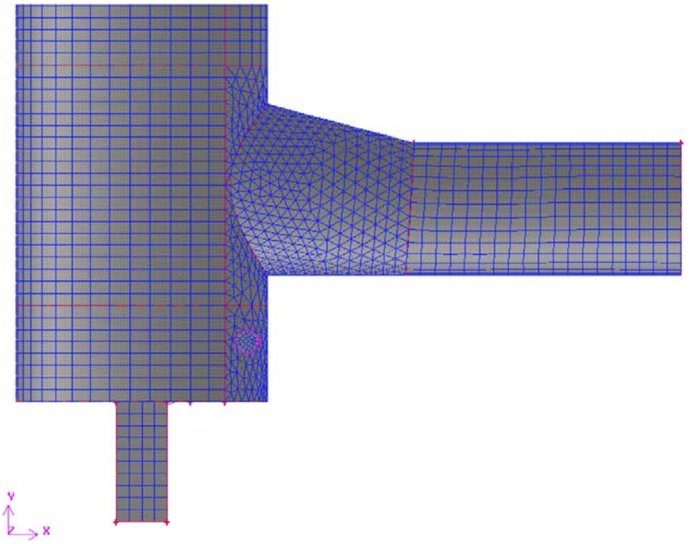

Fig. 5. Gridwork of the area in the vicinity of the quenching tank.

mixture of CO_2, H_2O, N_2 and O_2, with the following composition expressed as percentages of volume:

CO_2 9.0%, H_2O 18.1%, N_2 71.1% and O_2 1.8%.

3.4. Turbulence

In this case, the flow is turbulent, with varying velocity fields: the variations may be small-scale and high-frequency. An accurate turbulence analysis would be very costly, so various simulation models are generally employed.

Unfortunately, there is no turbulence model that can be considered to be the optimum for all types of problem: which model is selected depends on a number of factors, such as the physical flow-pattern, practical experience in each case, the required precision level and the availability of computational resources.

In this instance, the k–ε standard turbulence model was selected for the simulation. It is a semi-empirical 2-equation model based on turbulent kinetic energy (k) transportation and its dissipation rate (ε), which behaves reasonably well on fully-turbulent flows, where molecular viscosity has little effect.

3.5. CFD procedure scheme

Mathematical modelling using a CFD technique is a very strong and effective tool to simulate the flow and combustion in an industrial boiler [5–8].

The modelling was carried out using the Standard Fluent code version 6 [9,10] and predictions were validated against a set of data obtained in a chain furnace.

The numerical procedure used in CFD programs for the resolution of transportation differential equations is based on the application of finite-volume techniques [11–17], basically consisting of:

- Dividing the domain into discrete volumes using a computational grid.
- Integrating transportation equations into individual control-volumes in order to build algebraic equations for the dependent discrete variables, such as velocity, pressure, temperature and scalars.
- Linearising discrete equations and solving the linear equation system to calculate the actual values of the dependent variables.

This way an iterative resolution procedure is applied until established convergence criteria are reached for all the variables.

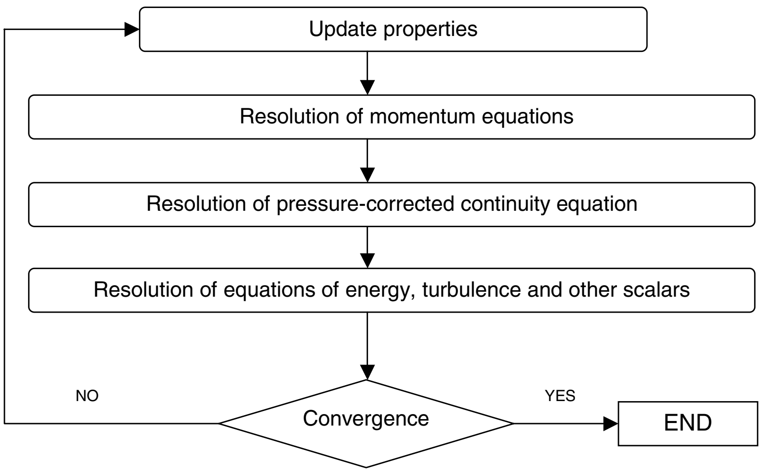

4. Results obtained from simulations

Fig. 6 shows the temperature contours obtained via the simulation, corresponding to the vertical plane of symmetry of the furnace in the vicinity of the lower connection. The temperature drop along the chain (represented by the central rectangular section of the figure) can be clearly seen, as can that of the gases in the area immediately above the quenching bath. Thus, at an elevation $z = 0.25$ m above the water tank, the average gas temperature is 400 K, whereas at $z = 0.5$ m, the average temperature is 750 K and at $z = 0.8$ m it rises to 970 K [18–23].

Fig. 7 represents gas paths for flows out from the lower connection. From this figure, it is evident that these gases do not penetrate sufficiently into the lower end of

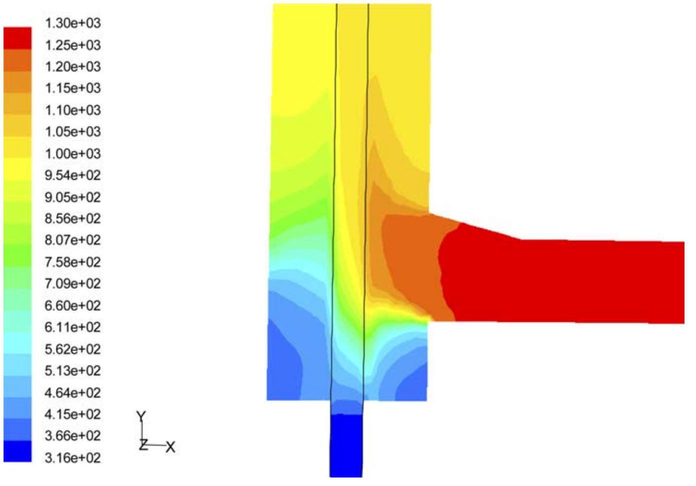

Fig. 6. Temperature contours at the furnace's lower connection.

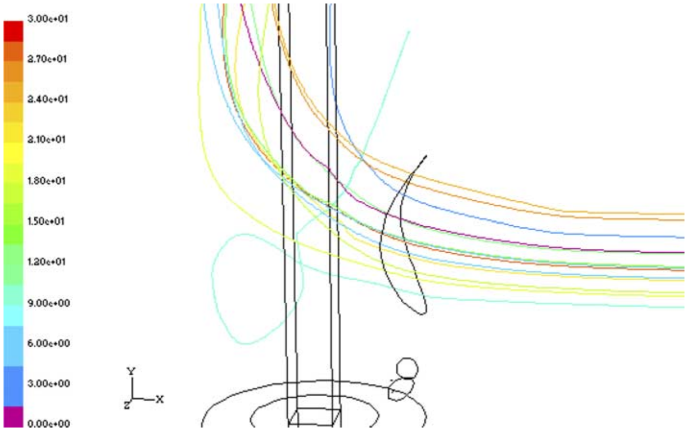

Fig. 7. Gas-flow paths coming from the lower connection.

the furnace, but clearly tend to rise along the furnace column. As a result, the furnace atmosphere at the lower end (i.e., just above the quenching tank) has a higher concentration of water vapour. Water takes heat from the adjacent areas to vaporise and heats up, gradually mixing with the exhaust gases in the flue. Evaporation and vapour-heating processes have a negative cooling effect on the chain, precisely in the final part of its run through the furnace.

Fig. 8 represents chain temperature profiles against elevations inside the furnace, in the downward movement towards the quenching tank. It can be seen that, in some sections, the temperature spread is wide. This is because hot gases from the furnace burners impinge on one side of the chain, whereas the other side is in contact with

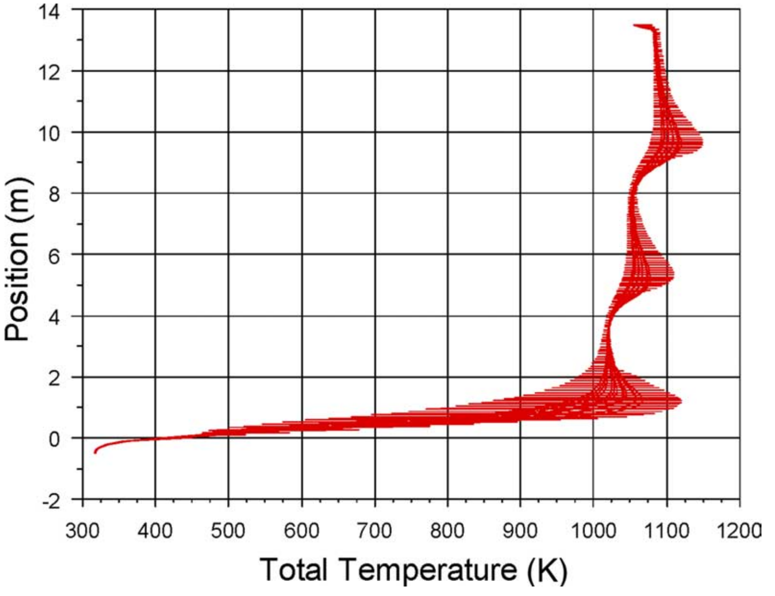

Fig. 8. Chain's temperature profile.

colder gas, generating a less even temperature distribution through the horizontal cross-section at the same elevation.

Also, the gradual cooling of the chain before reaching the hardening area (elevation 0 on the diagram) can clearly be seen: its temperature drops by around half at an elevation of one metre above the water level.

Results from the simulation are compared with temperature measurements taken during a furnace operating cycle by placing a number of thermojunctions in different

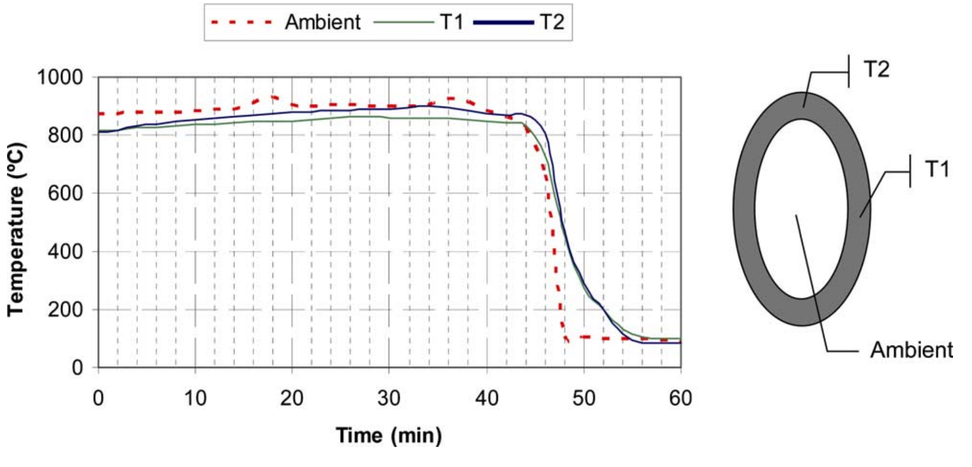

Fig. 9. Furnace temperature records.

positions on one chain link and recording temperatures as the chain moved through the furnace.

Fig. 9 represents the temperatures obtained from measurements at two points on the chain (T_1 on the shank and T_2 on the elbow) as well as the temperature inside the furnace, taken at the link's centre. The diagram shows the time-lapse between the moment the link is immersed in the water of the quenching tank and the minutes preceding immersion (i.e., for approximately the last 5 m of the furnace column).

Comparing Figs. 8 and 9, it can be clearly seen that the temperatures obtained from the measurements are within the range predicted by the simulation. It can thus be concluded that the results obtained from the numerical simulation are acceptable in terms of reliability and quality for the present analysis.

5. Proposal for improvement

Based on the above conclusions and after investigating other alternatives, a combined solution is proposed, consisting of redirecting part of the gas flow from the main combustion chamber toward the problem area, and, at the same time, removing part of the water vapour generated. The idea is to direct this flow against the lower part of the chain, thus increasing its temperature in the final part of the run before the chain enters the water, simultaneously removing the vapour generated by the entry of the chain into the quenching tank as quickly as possible.

To redirect the gases, two plates, measuring $550 \times 150 \times 10$ mm, are placed in the lower intake of gas from the main combustion chamber into the furnace. The upper plate is tilted at an angle of 20° and the lower plate at 30°. Gas baffled by the lower plate is intended to heat up the last 30 cm of chain before it enters the water and gas baffled by the upper plate is intended to heat up the 30 cm immediately above the area heated by the lower plate.

Water vapour is removed through a vent close to where it is generated, so as to avoid contact with the chain and the resulting temperature loss. To that end, a 20-cm diameter pipe is placed above the water level and below the hot gas intake. A negative pressure is created in this pipe by means of a fan, so as to allow water vapour to be sucked out together with part of the gases – see Fig. 10.

5.1. Gridwork

The chain is divided into 5888 elements. Gridwork is based on hexahedral elements, applying a MAP type grid-scheme. The combustion gas area contains 155,604 elements of the hexahedral and tetrahedral types. To make the gridwork easier, the furnace geometry is broken down, and different grid schemes (COOPER, MAP and T-GRID) are then applied, depending on the areas.

Figs. 11 and 12 show temperature fields for different furnace planes and at different cross-sections inside the area investigated, both for the gas atmosphere and the chain itself. Comparing this with the present operating conditions, it can be concluded that redirecting the gas flow has a substantial effect in terms of increasing

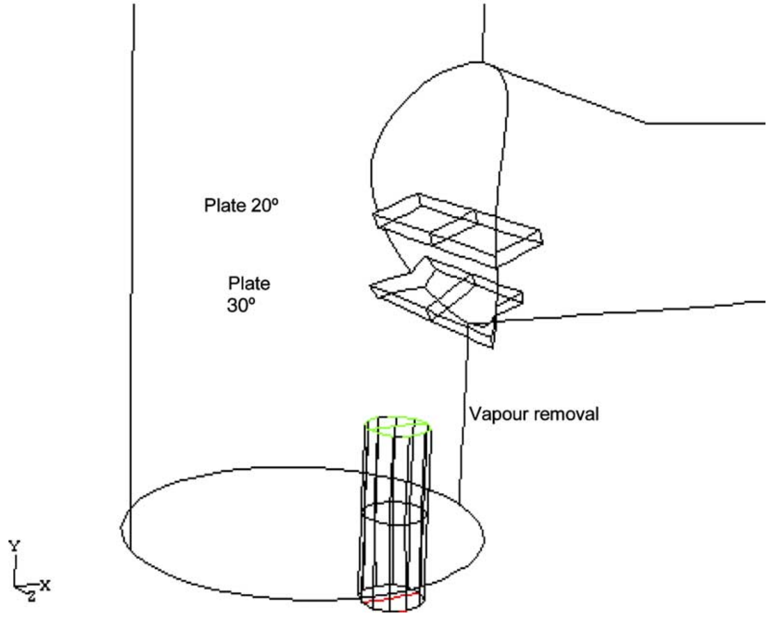

Fig. 10. Proposal for improvement of the hardening furnace.

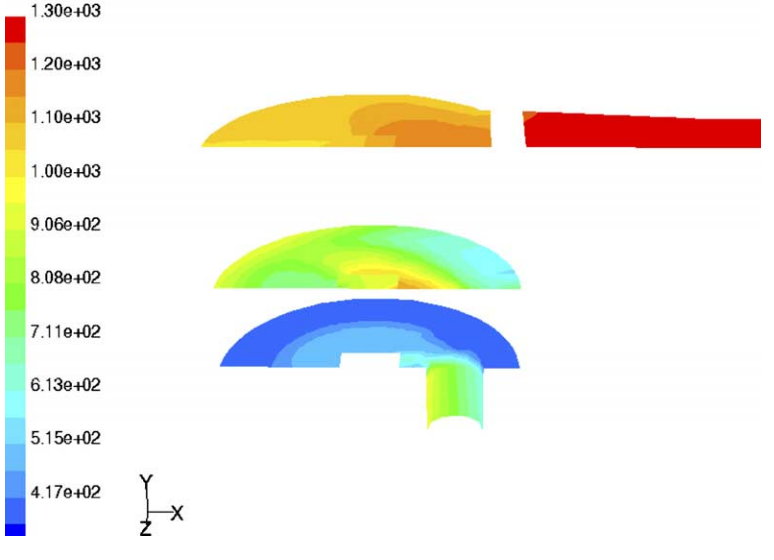

Fig. 11. Temperature contours at elevations $z = 0.25$, 0.5 and 0.8 m above the quenching tank.

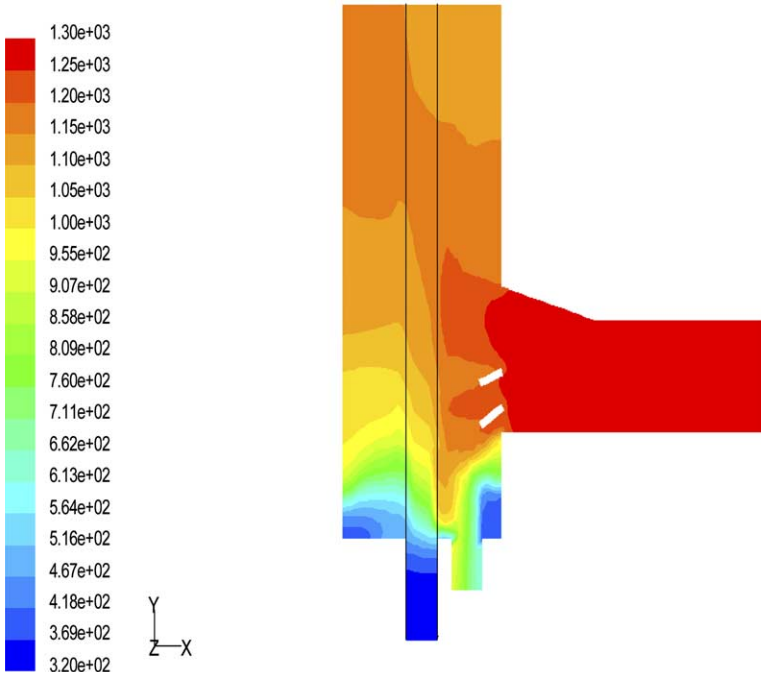

Fig. 12. Temperature (K) on the plane of the vertical symmetry at the furnace's lower connection.

the gas temperature in the lower part of the furnace, which changes the chain temperature accordingly.

Fig. 13 shows the paths of the gas from the combustion chamber. It can be appreciated that part of the flow of hot gases goes into the lower part of the furnace, thereby helping to heat it further and producing a slight overpressure that helps confine the water vapour generated in the quenching tank at the lower elevations.

This, together with the effect produced by the vapour-removing equipment, results in large amounts of vapour and colder gases being drawn out through the duct and removed from the furnace to the flue, as can be seen in Fig. 14, in which the vapour paths are depicted.

The end result is to increase the temperature of the chain along its downward movement through the furnace, and most significantly at the end of its run.

Indeed, a comparison of the temperature-profile diagram in Fig. 15 with the current operating conditions (Fig. 8) shows an increase in the cooling rate as well as a higher chain-temperature during the approach run and before quenching (elevation 0 in the figures).

It is also worth mentioning that the chain's temperature-distribution along its downward movement inside the column is more even. This reduction of the thermal gradient compared with current conditions can be explained as a consequence of the removal of the water vapour and a more homogenous furnace-atmosphere temperature.

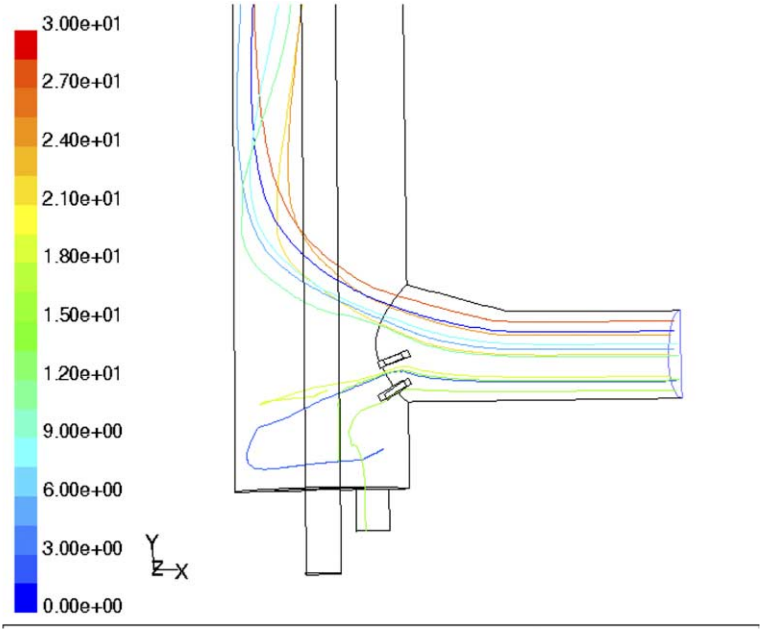

Fig. 13. Gas paths from the lower connection.

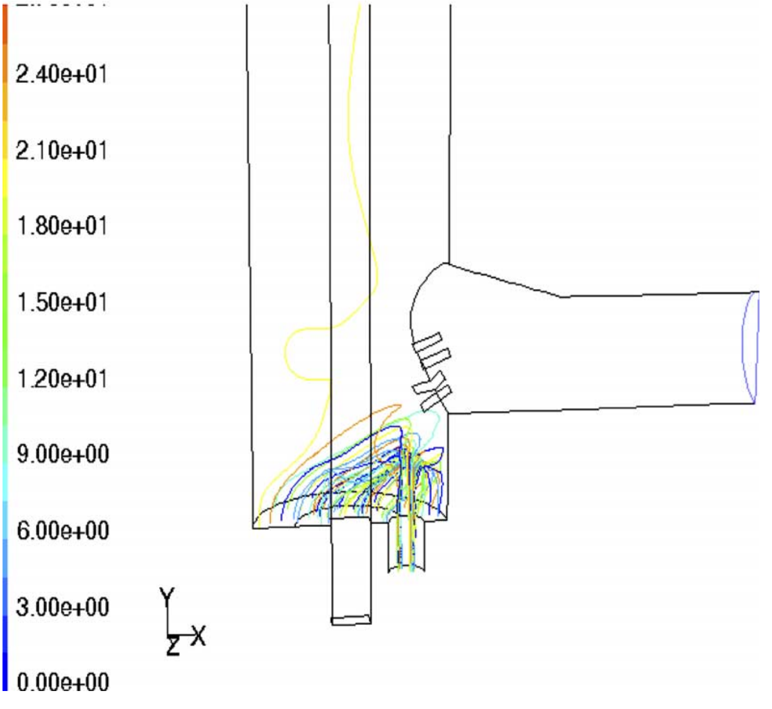

Fig. 14. Paths of the water vapour generated in the quench tank.

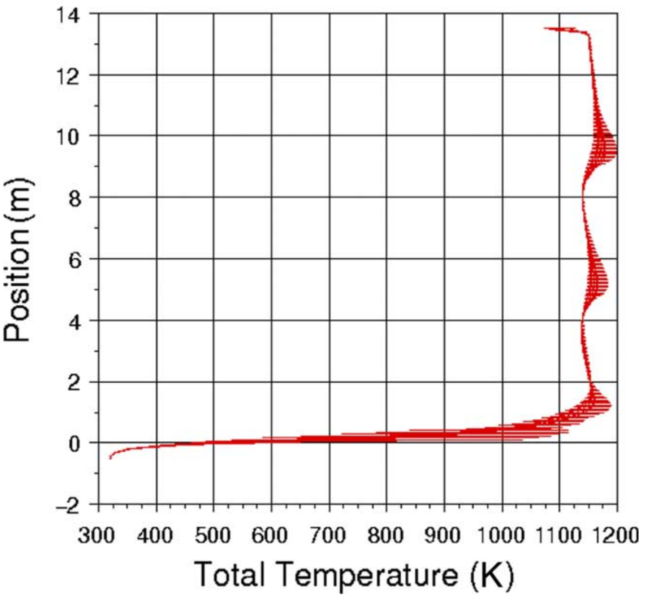

Fig. 15. Chain's temperature profile.

The results obtained in this investigation have been implemented on one of the furnaces at the company's plant in Bilbao. Operation has been found empirically to have improved significantly, thus improving the quality of the product manufactured. Fig. 16 shows the readings of experimental temperature-measurements taken by placing two thermojunctions on a link of chain and a third inside the furnace atmosphere after the proposed modifications were implemented.

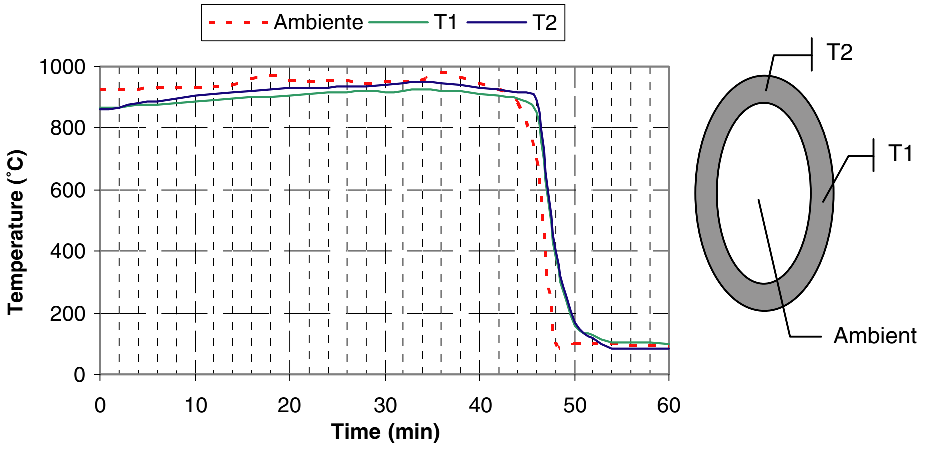

Fig. 16. Furnace's temperature records.

The trends observed during the simulation are corroborated by the thermal record. In comparison with previous conditions (Fig. 9), the following can be observed:

- In general, the chain temperature in the few last metres before entering the quenching tank has increased.
- Temperatures T_1 and T_2 have a narrower spread, so that temperatures inside the chain are more even, as shown in the simulation.
- The slope of the cooling curve is greatly increased, i.e., the chain temperature drop is quicker, thus increasing the hardening-process quality and as a result the quality of the end product.

6. Conclusions

This investigation has proved the enormous possibilities of CFD for analysing gas aerodynamics and heat-transfer processes inside furnaces. Specifically, a furnace for large chains with important flaws in the hardening process, due to which quick cooling of the chain was not possible, has been investigated.

A solution is proposed consisting of redirecting gases by means of two baffle plates placed in the lower gas intake from the main combustion chamber, and a duct through which vapours produced when quenching the chain are drawn off by means of a fan.

After the proposed modifications the chain temperature rose significantly, and quicker cooling and better hardening became possible.

References

[1] Gan G, Riffat S. Numerical determination of energy losses at duct junctions. Appl Energy 2000;67(3):331–40.

[2] Stanley Mumma, Mahank T, Yu-Pei Ke. Analytical determination of duct fitting loss-coefficients. Appl Energy 1998;61(4):224–9.

[3] Stephenson PL. Mathematical modelling of semi-anthracite combustion in a single-burner furnace. Fuel 2003;82:2069–73.

[4] Ghobadian A, Lee F, Stephenson PL. Validation of the coal combustion capability in the Star-CD code, I Mech E Seminar on CFD – technical developments and future trends, London, 13–14 December 1999.

[5] Falcitelli M, Pasini S, Tognotti L. Modelling practical combustion systems and predicting NO*x* emissions with an integrated CFD-based approach. Comput Chem Eng 2002;26:1171–83.

[6] Benedetto D, Gelmini A, Mola A, Pasini S, Santero A. Thermofluidodynamic 3D modelling of glass-melting furnaces for combustion optimisation and emission reduction. In: Fifteenth ATIV meeting – glass industry, Parma, Italy, 15–17 September 2000.

[7] Bhasker C. Simulation of air flow in the typical boiler windbox segments. Adv Eng Software 2002;33:793–804.

[8] Chow WK. Numerical studies of airflows induced by mechanical ventilation and air-conditioning (MVAC) systems. Appl Energy 2001;68(2):135–59.

[9] Knudsen S, Furbo S. Thermal stratification in vertical mantle heat-exchangers with application to solar domestic hot-water systems. Appl Energy 2004;78(3):257–72.
[10] Rhine JM, Tucker RJ. Modelling of gas-fired furnaces and boilers. New York: McGraw-Hill; 1991.
[11] Mull Jr TV, Hopkins MW, White DG. Numerical-simulation models for a modern boiler design. Paper No. BR-1627. Power-Gen, International, Florida, 1996.
[12] Dong W, Blasiak W. CFD modeling of ecotube system in coal and waste grate combustion. Energ Convers Manage 2001;42:1887–96.
[13] Fluent Inc. FLUENT User's Guide. Fluent Inc., Lebanon (NH, USA), December 2001.
[14] Fluent Inc. Gambit user's guide, e. Fluent Inc., Lebanon (NH, USA), 1998.
[15] Anderson DA, Tannehill JC, Pletcher RH. Computational fluid mechanics and heat transfer. New York: Hemisphere, Taylor and Francis Group; 1984.
[16] Versteg HK, Malalasekera W. An introduction to computational fluid-dynamics. In: The finite-volume method. New York: Wiley; 1995.
[17] Von Karman Institute for fluid dynamics. Introduction to the modelling of turbulence. Brussels: Von Karman Institute; 1991.
[18] Incropera FP, Dewitt DP. Fundamentals of heat and mass transfer. New York: Wiley; 1996.
[19] White K, Probert SD. Heat transfers in treatment furnaces. Appl Energy 1991;38(4):293–323.
[20] Blokh AG. Heat transfer in steam boiler furnaces. Berlin: Springer; 1984.
[21] Guyer EC. Handbook of applied thermal design. New York: McGraw Hill; 1989.
[22] Wilcox DC. Turbulence modelling for CFD. La Canada: DCW Industries Inc.; 1993.
[23] Jaulria Y, Torrance KE. Computational heat-transfer. New York: Hemisphere Publishing Corporation; 1986.